Nuclear Materials and Energy 15 (2018) 97–102

Contents lists available at ScienceDirect

Nuclear Materials and Energy

journal homepage: www.elsevier.com/locate/nme

Ratcheting behavior of Eurofer97 at 550 °C

Zhang Kuo*, Jarir Aktaa

Karlsruhe Institute of Technology (KIT), Institute for Applied Materials, Hermann-von-Helmholtz-Platz 1, 76344 Eggenstein-Leopoldshafen, Germany

ARTICLE INFO

Keywords:
Eurofer97
Ratcheting behavior
Constitutive model
550 °C

ABSTRACT

The components in reactor are usually exposed to cyclic loading caused by frequent startups, shutdown and load fluctuations which lead to ratcheting effect. Eurofer97 is a structural material candidate for in-vessel components of future fusion reactor. To investigate the ratcheting behavior of Eurofer97, uniaxial stress-controlled cyclic loading tests are performed at 550 °C. Ratcheting rates under various loading conditions, including various peak stresses, stress ratios and stress rates are determined to build the database of Eurofer97 for future application in the blankets of fusion reactor. An already developed unified visco-plastic constitutive model for mod.9Cr-1Mo FM steels is further applied to adapt the ratcheting behavior of Eurofer97. The developed model describes both cyclic softening in strain-controlled LCF tests and its impact on the ratcheting behavior of mod.9Cr-1Mo FM steel fairly good, at both room temperature and 550 °C. Verifying whether the current model can also describe the ratcheting behavior of Eurofer97 is a further aim of the work reported here.

1. Background and introduction

Eurofer97 is considered as one of the candidates for structural material of future fusion reactor [1–3]. This steel belongs to the group of Reduced-Activation Ferritic-Martensitic (RAFM) steels. Comparing RAFM steels to other conventional ferritic-martensitic (FM) steels such as mod. 9Cr-1Mo FM steel (P91), typical steel alloying elements Mo, Nb, Ni, Cu and N are either eliminated or minimized. For instance, molybdenum is replaced by tungsten [4–8] and niobium is replaced by tantalum [4,5].

The frequent startups, shutdowns, and load changes imposed by cycling duty lead to thermo-mechanical fatigue of structural material in nuclear power plants [9]. The same loading condition is also expected for Eurofer97 which lead to ratcheting effect. However, there is currently a lack of satisfying design rule for Eurofer97 concerning the ratcheting. Therefore the study of the ratcheting behavior of Eurofer97 is included in the research project for future fusion reactor and a priority is given to the test matrices for the characterization of the ratcheting behavior of Eurofer97.

According to a previous study on the ratcheting of P91 [10], it is believed that the Eurofer97 steel would have similar mechanical characteristic as P91, including cyclic softening and ratcheting. Cyclic softening of Eurofer97 has already been verified in previous studies [2, 11] while the data for the ratcheting of Eurofer97 are still missing.

2. Material and testing

In this research, strain-responses of cylindrical Eurofer97-2 specimens are recorded under uniaxial stress-controlled cyclic loading. The material is normalized at 980 °C for 30 min and tempered at 760 °C for 90 min. The specimens are firstly cut by electrical discharge machining (EDM). Afterwards, the specimens are further processed by turning and polishing to a nominal diameter of 8.8 mm and gauge length of 23 mm, as is shown in Fig. 1.

The chemical composition of Eurofer97-2 follows the same specification of the first batch. The second batch is produced in a way of massive industrial production. The specified chemical compositions are listed in Table 1:

Similar to the former ratcheting tests on P91 [10], the tests on Eurofer97 are performed under true-stress control. The reason is that, the strain response under true-stress control will reflect the pure material properties, without structural influence. Since the total strain in ratcheting can be more than 1%, the difference between engineering stress and true stress is not negligible. Therefore these experimental data with true-stress control are more suitable to be directly applied in the constitutive modeling required for finite-element simulation.

The principle of true-stress control is as following: The real time axial deformation ΔL is taken to modify the output signal which controls the loading F on the specimen, to adapt the reduced cross section $A' = A/(1 + \varepsilon)$ of the specimen with $\varepsilon = \Delta L/L$. The load F of the hydraulic testing machine is linearly related to the modified output signal. Therefore the modified load is $F' = F/(1 + \varepsilon)$, which corresponds to the

* Corresponding author.
E-mail address: kuo.zhang@kit.edu (K. Zhang).

https://doi.org/10.1016/j.nme.2018.03.003
Received 13 December 2017; Received in revised form 5 March 2018; Accepted 9 March 2018
Available online 21 March 2018

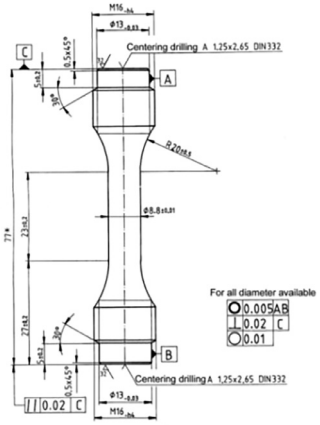

Fig. 1. Cylindrical specimen for uniaxial test.

Table 1
Specified chemical compositions of Eurofer97 [12].

	Eurofer97 specified (wt%)
C	0.09–0.12 [0.11]
Cr	8.5–9.5 [9.0]
W	1.0–1.2 [1.1]
Mn	0.20–0.60 [0.40]
V	0.15–0.25
Ta	0.10–0.14 [0.12]
N_2	0.015–0.045 [0.030]
P	< 0.005
S	< 0.005
B	< 0.001
O_2	< 0.01
Nb	< 0.001
Mo	< 0.005
Ni	< 0.005
Cu	< 0.005
Al	< 0.01
Ti	< 0.01
Si	< 0.05
Co	< 0.005

reduced cross section *A′*.

The experiments are performed following the test matrices in Table 2. Following sub-table a), tests with the same stress ratio −0.9 are performed. The peak stresses range between 250 MPa and 350 MPa. The mean stresses change accordingly. In the previous test matrix for P91 [10], this group of tests were performed with the same mean stress. However, as revealed by the ratcheting of P91, the highest ratcheting rate for a certain peak stress appears at a stress ratio between −0.95 and −0.9, it is therefore more reasonable to keep the stress ratio instead of keeping the mean stress as a constant, to find approximately the highest ratcheting rate for each peak stress.

Note that the term “ratcheting rate” is defined as the difference of mean strain from the current loading cycle to the previous loading cycle. For instance, if the stress-strain hysteresis loop stays, the ratcheting rate is then zero. The term “average ratcheting rate” is therefore the mean strain of the current loading cycle divided by the corresponding cycle number.

Following the sub-table b), tests are performed with the same peak stress 300 MPa and various stress ratios, ranging from −1 to 0. Additional two tests are done with stress rates of 10 and 250 MPa/s to illustrate the visco-plasticity of the material, as listed in sub-table c). The default stress rate for all the other tests is 50 MPa/s.

3. Experiment results

The load and the extension of the extensometer are recorded by every 0.02 s. Accordingly, the true stress and true strain are calculated and analyzed. The experiment results are collected and illustrated in Figs. 2–6.

Fig. 2 shows the stress-strain hysteresis loops of four different cycles (1st, 200th, 400th and 600th cycle) of one of the ratcheting tests. The stress alternates between 300 MPa and −270 MPa with stress rate of 50 MPa/s at the temperature 550 °C. The mean stress is therefore 15 MPa in tensile direction. Obviously, the strain accumulates in the direction of the mean stress, which is a typical ratcheting behavior. The widths of the hysteresis loops also increase by the accumulating cycle number, which reveals the cyclic softening of the material. On the other hand, the cyclic softening accelerates the ratcheting rate.

After collecting the middle strain of each cycle, diagrams as the one in Fig. 3 can be drawn. The middle strain is now named as “ratcheting strain”. This diagram shows the relationship between the ratcheting strain and the cycle number of seven tests. The peak stresses range between 250 MPa and 350 MPa and the stress ratio is kept to −0.9.

The ratcheting strains of the tests with peak stress 285 and 250 MPa are hardly shown in Fig. 3 since they are relatively negligible. Therefore another diagram is generated and shown in Fig. 4, where the average ratcheting rates until the accumulated strain reaches 3% or the cycle number reaches 10,000, whatever comes first, are plotted. A linear relationship is found for the peak stresses from 285 to 350 MPa. The ratcheting rate for peak stress of 250 MPa is less than 10^{-7} per cycle and is hence negligible. It is suggested that the ratcheting is excited when peak stress is larger than 250 MPa at 550 °C.

Another group of tests are performed according to Table 2b) and the average ratcheting rates are summarized in Fig. 5. In the same diagram, the corresponding test results of P91 are also drawn, to compare with those of Eurofer97. Obviously the highest ratcheting rates appear at stress ratios between −0.95 and −0.9 for both materials. The ratcheting is relatively negligible when the stress ratio is between −0.5 and 0, since the stress ranges is too small to cause inelastic strain. Note that the peak stress for P91 is kept at 325 MPa and the peak stress for Eurofer97 is kept at 300 MPa, while their ratcheting rates are comparable. Therefore it comes to the conclusion, that P91 steel is tougher than Eurofer97 in terms of ratcheting.

After another two tests with stress rates 10 & 250 MPa/s are performed, the visco-plasticity of the material is revealed. The relationships between ratcheting strain and the cycle number of the three tests are illustrated in Fig. 6. After calculating the average ratcheting rates before the strain reaches 1%, 2% and 3% of these three tests, it is revealed that the ratcheting rate of the tests with 50 MPa/s is approximately two times higher than that with 250 MPa/s, while for P91 steel, the corresponding value is only 36% higher. This suggests that the mechanical properties of Eurofer97 are more time-dependent than that of P91. In other words, the Eurofer97 has higher viscosity than P91.

4. Modeling and simulation

4.1. Constitutive model

A constitutive model was previously developed to simulate the ratcheting of P91 at room temperature and 550 °C [10]. The ratcheting strains in the previous simulation ideally match the ratcheting strains in the experiments, in terms of the following three points:

1. The larger peak stress leads to higher ratcheting rate.
2. Highest ratcheting rate appears with stress ratio between −0.95 and −0.9.
3. Increasing ratcheting rate with decreasing stress rate.

This model in [10] is a modification of Aktaa–Schmitt model [2], which originates from the Chaboche model [13, 14] considering creep and plasticity as arising from the same dislocation source [15]. Aktaa–Schmitt model has additional description of cyclic softening,

Table 2
Stress-controlled uniaxial tests on Eurofer97 at 550 °C.

a) Influence of peak stress

σ_{max} [MPa]	350	335	325	315	300	285	265	250
σ_{min} [MPa]	-315	-301.5	-292.5	-283.5	-270	-256.5	-238.5	-225
Stress ratio	-0.9							
σ_{mean} [MPa]	17.5	16.75	16.25	15.75	15	14.25	13.25	12.5
$\dot{\sigma}$ [MPa/s]	±50							

b) Influence of mean stress/stress ratio

σ_{max} [MPa]	300							
σ_{min} [MPa]	0	-150	210	-240	-270	-285	-294	-300
Stress ratio	0.0	-0.5	-0.7	-0.8	-0.9	-0.95	-0.98	-1.0
σ_{mean} [MPa]	150	75	45	30	15	7.5	3	0
$\dot{\sigma}$ [MPa/s]	±50							

c) Influence of stress rate

σ_{max} [MPa]	300		
σ_{min} [MPa]	-270		
$\dot{\sigma}$ [MPa/s]	±10	±50	±250

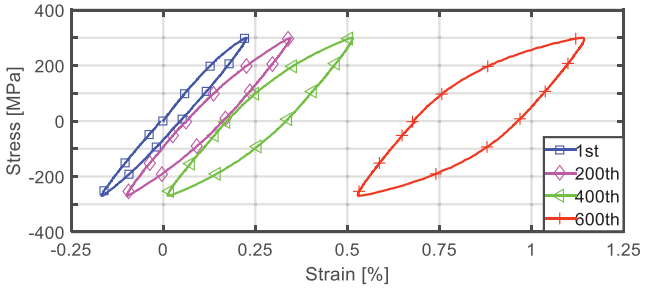

Fig. 2. Stress-strain hysteresis loops of several loading cycles in the ratcheting test, with max. stress 300 MPa, min. stress −270 MPa, stress rate 50 MPa/s.

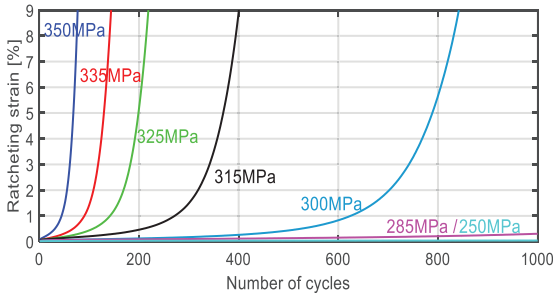

Fig. 3. Ratcheting strain vs. number of cycles of ratcheting tests with various peak stresses from 250 MPa to 350 MPa. Stress ratios are −0.9, stress rates are 50 MPa/s.

typically for the RAFM steels, e.g. Eurofer97. A further modification was made in [10] with an additional back stress component to avoid the overestimation of ratcheting rate due to the Armstrong-Frederick dynamic recovery rule [15] used in the Chaboche model.

On the other hand, the existing model has strongly reduced the number of back stress components comparing to other modeling approaches for ratcheting [16–21], from four, eight even 12 back stress components to only two. One back stress component controls the fitting on the stress-strain hysteresis loops, while the other controls the fitting on the ratcheting rates.

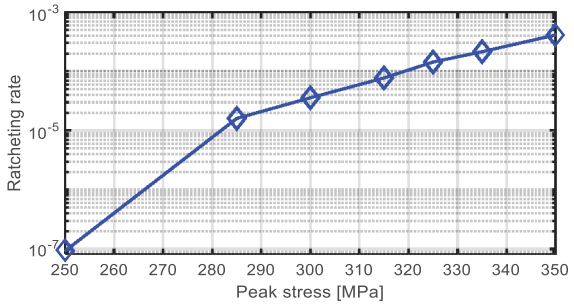

Fig. 4. Average ratcheting rates vs. peak stresses with various peak stresses from 250 MPa to 350 MPa. Stress ratios are −0.9, stress rates are 50 MPa/s.

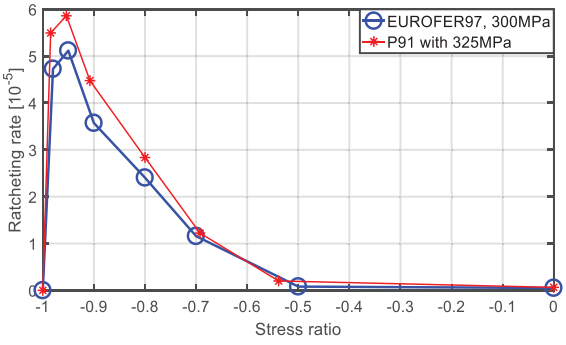

Fig. 5. Average ratcheting rates vs. stress ratios with various stress ratios from −1 to 0. Peak stresses are 300 MPa for Eurofer97 and 325 MPa for P91.

The equations for the constitutive model are listed in Table 3.

E, k, Z, n, h, c, r_{ψ_s}, ψ_r, m_{ψ_s}, $\psi_{s,\infty}$, H_1, C_1 R_1, m_1, H_2, r_2, R_2, m_2 and n_2 are material- and temperature-dependent parameters. ψ_1 and ψ_2 are the two state variables to describe the cyclic softening. Ω_1 and Ω_2 are the two back stress components. The equation of Ω_1 Eq. (8) controls the shapes of the simulated stress-strain hysteresis loops. The equation of Ω_2 Eq. (9) controls the ratcheting rate. In the modeling approach for P91, most of the efforts in the modeling approach were spent on the parameter

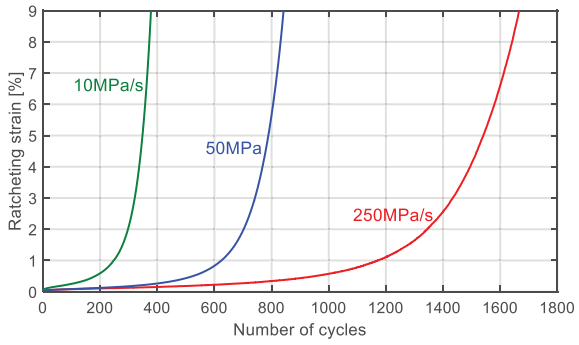

Fig. 6. Average ratcheting rates vs. stress rates with various stress rate 10, 50 and 250 MPa/s. Peak stresses are 300 MPa.

Table 3
Equations of the constitutive model.

$$\dot{\varepsilon} = \dot{\varepsilon}^{in} + \dot{\varepsilon}^{el} \quad (1)$$

$$\dot{\varepsilon}^{el} = \frac{\dot{\sigma}}{E} \quad (2)$$

$$\dot{\varepsilon}^{in} = \left\langle \frac{|\sum| - k}{Z} \right\rangle^{n} \mathrm{sgn}(\sum) \; with \sum = \frac{\sigma}{\psi} - \Omega \quad (3)$$

$$\psi = \psi_1 + \psi_2, \; with \; \psi_1(t=0) = 0 \; and \; \psi_2(t=0) = 1 \quad (4)$$

$$\dot{\psi}_1 = -h|\dot{\varepsilon}^{in}| \quad (5)$$

$$\dot{\psi}_2 = c(1 - \psi_{s,\infty} - \psi_2)|\dot{\varepsilon}^{in}| - r_\psi|\psi_2 - \psi_r|^{m_\psi - 1}(\psi_2 - \psi_r) \quad (6)$$

$$\Omega = \Omega_1 + \Omega_2 \quad (7)$$

$$\dot{\Omega}_1 = H_1\dot{\varepsilon}^{in} - C_1\Omega_1|\dot{\varepsilon}^{in}| - R_1|\Omega_1|^{m_1 - 1}\Omega_1 \quad (8)$$

$$\dot{\Omega}_2 = H_2\dot{\varepsilon}^{in} - |\Omega_2|^{n_2 - 1}\Omega_2\left\langle \dot{\varepsilon}^{in}\frac{\Omega_2}{r_2} \right\rangle - R_2|\Omega_2|^{m_2 - 1}\Omega_2 \quad (9)$$

fitting for Ω_2 and the modification of Eq. (9), especially the dynamic recovery part (the middle part on the right hand side of Eq. (9)).

4.2. Modeling for Eurofer97

Since the mechanical behavior of Eurofer97 is similar to P91 steel, as has been discussed in Section 3, it is not necessary to modify the equations. However it is still necessary to modify the parameter values, because Eurofer97 is weaker than P91 in terms of ratcheting, as shown in Fig. 5.

The experimental data of strain-controlled low cycle fatigue (LCF) tests of the previous research on Eurofer97 [2] are also put into consideration, together with the tests following Table 2. For the Aktaa–Schmitt model in [2], a group of parameter values are already fitted for LCF tests of Eurofer97 at 550 °C. Although the cyclic softening of the material has been ideally expressed by this model, the corresponding simulated ratcheting overestimated the ratcheting rate due to the application of Armstrong-Frederick kinematic hardening rule [15]. Although Armstrong-Frederick kinematic hardening rule has successfully expressed the material response under strain-controlled loading, it always leads to overestimation of the strain accumulation under stress-controlled loading [16–21].

Due to the unsatisfying modeling behavior of Aktaa–Schmitt model in [2] for ratcheting of Eurofer97, the model developed in [10] shall be applied. Unfortunately all the parameters values, except Young's modulus, have to be re-fitted, because no convincing physical measurement exists for these parameters. For instance, the values of parameters *k, Z, n,* which dominate the visco-plasticity behavior in the simulation, cannot give a satisfying simulation result for the three ratcheting tests with stress rates of 10, 50, 250 MPa/s. On the other hand, different combinations of parameter values of *k, Z, n,* H_1, C_1 can have similar modeling performance for LFC tests, but only few can have, at the same time, satisfying modeling performance for ratcheting tests.

Therefore all the parameter values must be fitted, by performing the simulation of LCF tests and ratcheting tests with various loading condition together. In other words, all available experiments shall be simulated, to fit all the parameter values.

Table 4
Fitted parameter values for the constitutive model in Table 3. Values for P91 at 550 °C are listed to compare with the values of Eurofer97.

	Eurofer97	P91
E (MPa)	153,890	173,130
k (MPa)	25	65.2917
Z(MPa s$^{1/n}$)	365	295.332
n	25	47.911
H_1 (MPa)	135,980	55,479.1
C_1	1357.5	638.752
R_1(MPa$^{1-m_1}$s^{-1})	1×10^{-10}	3.32178×10^{-3}
m_1	5.255	2.08665
H_2 (MPa)	68,750	13,853.8
r_2	12.5	0.21402
R_2(MPa$^{1-m_2}$s^{-1})	0.025	3.68420×10^{-6}
m_2	3.004	0.017228
n_2	7.15	0.707266
h	1.6×10^{-3}	1.98945×10^{-2}
c	2.5	3.85381
r_ψ (s^{-1})	3.388×10^{-4}	8.86652×10^{-5}
ψ_r	0.99	0.850816
m_ψ	1	1.47506
$\psi_{s,\infty}$	0.45	0.206453

4.3. Simulation results

A group of parameter values with satisfying simulation results is determined after the calculation in MATLAB. The fitting programs are based on a fortran program MINUIT developed at CERN [22]. The main field of usage of MINUIT is statistical data analysis of experimental data recorded at CERN. The fitted parameter values are listed in Table 4.

The parameter fitting is started by inheriting the values of P91 steel from the previous study [10] as the initial values for the program MINUIT. However the fitting ends up at a group of values, which are very different from the values for P91. Several differences from the mechanical point of view are summarized as following:

1. As mentioned in the end of Section 3 of this report, the mechanical properties of Eurofer97 are more time-dependent than that of P91. Therefore the value of parameter n should be lower for Eurofer97. The value of parameter Z should be changed accordingly.
2. In the strain-controlled LCF tests, the peak stresses decrease rapidly in the initial phase of the lifetime, followed by a saturated steady-decreasing phase. The ratio between the peak stress in the first loading cycle and the peak stress in the cycle by the end of initial rapid-decreasing phase, is controlled by the parameter $\psi_{s,\infty}$. Since the peak stresses of Eurofer97 decrease to a lower degree in this initial rapid-decreasing phase, the value of $\psi_{s,\infty}$ should be higher for Eurofer97.
3. The value of parameter h controls the slope of the decreasing peak stresses in the steady-decreasing phase of the strain-controlled LCF tests. The value of h for P91 steel is too high for Eurofer97, since the peak stresses of Eurofer97 decrease slower in the saturated steady-decreasing phase.

Due to these above mentioned differences between P91 and Eurofer97, a very different group of parameter values is found for Eurofer97. It comes to the conclusion, that although the same constitutive model is able to describe the mechanical behavior of these two steels, they cannot share the similar parameter values. Note that the Young's modulus 153,890 MPa follows the measured value in the report [2] and it fits the current experimental data of Eurofer97-2nd batch.

Fig. 7 shows the comparison of ratcheting rates in simulations and

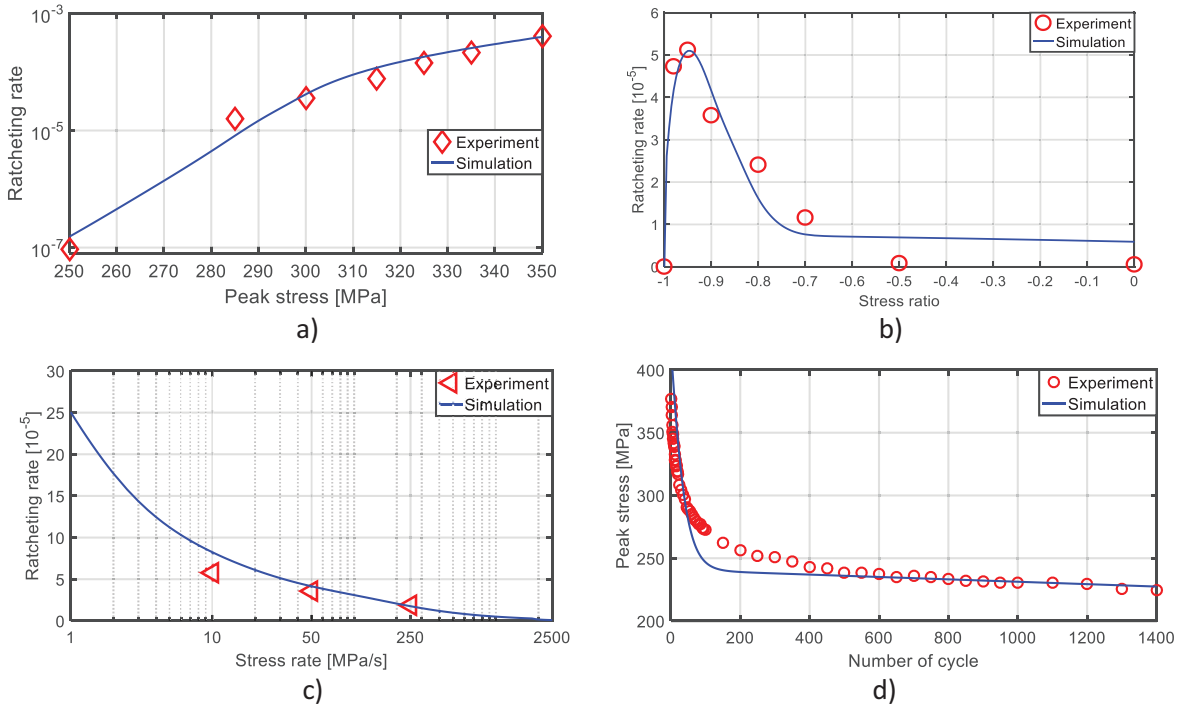

Fig. 7. Simulated average ratcheting rates comparing with experimental results, together with a simulated LCF test.

experiments, together with a simulated LCF test in sub-figure d). Three sub-figures a), b) and c) correspond to the three sub-tables in Table 2. The average ratcheting rates, both in experiments (red markers) and in simulation (blue curves) are those before the accumulated strain reaches 3% or the cycle number reaches 10,000, whatever comes first.

The simulated ratcheting rates shown in Fig. 7a) are calculated by each 1 MPa, from 250 MPa to 350 MPa. As can be seen, the agreement between model and material responses is quite well. Hence this model (in Table 3) is able to predict ratcheting rates under loadings in a very large range, yielding very high to relatively negligible ratcheting rates at 550 °C.

The simulated ratcheting rates shown in Fig. 7b) are calculated by each 0.002 of stress ratio, from −1 to −0.5, and by each 0.05, from −0.5 to 0. It is clear that the simulated ratcheting rate reaches its maximum at a stress ratio between −0.95 and −0.9, and the simulated rates are relatively negligible with stress ratios between −0.5 and 0, as the same as in the experiments. The matching between the model and material responses is satisfying.

The simulated ratcheting rates shown in Fig. 7c) are calculated by each 0.1 MPa/s from 1 to 50 MPa/s, each 0.5 MPa/s until 500 MPa/s and each 100 MPa/s until 2500 MPa/s. As can be seen, the experimental data at 10, 50 and 250 MPa/s (red triangles) correspond to the simulated rates (blue curve) quite well. Therefore this model (in Table 3) is also able to predict ratcheting rates under loadings with various loading rates, to describe the visco-plasticity of the material.

On the other hand, the simulated LCF test with strain amplitude 0.5%, as shown in Fig. 7d), also matches the experiment very well. The simulated peak stresses (blue curve) decrease rapidly in the initial stage and come to a steady decreasing phase afterwards until the fracture, as the same as the experiment. Hence the model can still simulate strain-controlled LCF test in a satisfying way.

5. Conclusion

The isothermal uniaxial ratcheting behavior of Eurofer97 at 550 °C is investigated by performing stress-controlled cyclic tests with various loading conditions. The ratcheting behavior is compared with the experimental data of mod.9Cr-1Mo ferritic martensitic steel P91. The parameter values in the previously developed constitutive model are fitted with the test data of Eurofer97, to check whether the existing model can describe the ratcheting behavior of Eurofer97.

After the above mentioned works, it comes to the following conclusions:

1. The ratcheting behavior of Eurofer97 is comparable to mod.9Cr-1Mo ferritic martensitic steel P91, although P91 is relatively tougher in terms of ratcheting.
2. The previously developed constitutive model can describe the ratcheting behavior of Eurofer97 at 550 °C:
   a) Higher ratcheting rate with higher peak stress
   b) Highest ratcheting rate with stress ratio between −0.95 and −0.9
   c) Increasing ratcheting rate with decreasing stress rate.

Acknowledgment

This work is carried out within the R&D Nuclear Fusion Program of the Karlsruhe Institute of Technology (KIT).

References

[1] A. Hishinuma, A. Kohyama, R.L. Klueh, D.S. Gelles, W. Dietz, K. Ehrlich, Current status and future R&D for reduced-activation ferritic/martensitic steels, 1998, 258–263, Part 1 (1998) 193–204.
[2] J. Aktaa, R. Schmitt, High temperature deformation and damage behavior of RAFM steels under low cycle fatigue loading: experiments and modeling, Fusion Eng. Des. 81 (2006) 2221–2231.
[3] V.B. Oliveira, H.R.Z. Sandim, D. Raabe, Abnormal grain growth in Eurofer-97 steel in the ferrite phase field, J. Nucl. Mater. 485 (2017) 23–38.
[4] C.-Y. Hsu, T.A. Lechtenberg, Microstructure and mechanical properties of uni-rradiated low activation Ferritic steel, J. Nucl. Mater. 141–143 (Part 2) (1986) 1107–1112.
[5] R.L. Klueh, A.T. Nelson, Ferritic/martensitic steels for next-generation reactors, J. Nucl. Mater. 371 (2007) 37–52.
[6] H. Kayano, H. Kurishita, A. Kimura, M. Narui, M. Yamazaki, Y. Suzuki, Charpy impact testing using miniature specimens and its application to the study of irradiation behavior of low-activation ferritic steels, J. Nucl. Mater. 179–181 (Part 1) (1991) 425–428.
[7] M. Yamanouchi, M. Tamura, H. Hayakawa, A. Hishinuma, T. Kondo, Accumulation of engineering data for practical use of reduced activation ferritic steel: 8%Cr-2%W-

0.2%V-0.04%Ta-Fe, J. Nucl. Mater. 191–194 (Part B) (1992) 822–826.
[8] F. Abe, T. Noda, H. Araki, S. Nakazawa, Alloy composition selection for improving strength and toughness of reduced activation 9Cr-W steels, J. Nucl. Mater. 179–181 (Part 1) (1991) 663–666.
[9] J.F. Henry, Growing experience with P91 T91 forcing essential code, Combined Cycle Journal, First Quarter (2005).
[10] K. Zhang, J. Aktaa, Characterization and modeling of the ratcheting behavior of the ferritic–martensitic steel P91, J. Nucl. Mater. 472 (2016) 227–239.
[11] M.F. Giordana, P.F. Giroux, I. Alvarez-Armas, M. Sauzay, A. Armas, Micromechanical modeling of the cyclic softening of EUROFER 97 steel, Procedia Eng 10 (2011) 1268–1273.
[12] A. Möslang, E. Diegele, M. Klimiankou, R. Lässer, R. Lindau, E. Lucon, E. Materna-Morris, C. Petersen, R. Pippan, J.W. Rensman, M. Rieth, B.v.d. Schaaf, H.C. Schneider, F. Tavassoli, Towards reduced activation structural materials data for fusion DEMO reactors, Nuclear Fusion 45 (2005) 649–655.
[13] J.L. Chaboche, G. Cailletaud, On the calculation of structures in cyclic plasticity or viscoplasticity, Comput. Struct. 23 (1986) 23–31.
[14] J.L. Chaboche, On some modifications of kinematic hardening to improve the description of ratchetting effects, Int. J. Plasticity 7 (1991) 661–678.
[15] C.O. Frederick, P.J. Armstrong, A mathematical representation of the multiaxial Bauschinger effect, Mater. High Temp. 24 (2007) 1–26.
[16] N. Ohno, J.D. Wang, Kinematic hardening rules with critical state of dynamic recovery, part I: formulation and basic features for ratchetting behavior, Int. J. Plasticity 9 (1993) 375–390.
[17] N. Ohno, J.D. Wang, Kinematic hardening rules with critical state of dynamic recovery, part II: application to experiments of ratcheting behavior, Int. J. Plasticity 9 (1993) 391–403.
[18] M. Abdel-Karim, N. Ohno, Kinematic hardening model suitable for ratchetting with steady-state, Int. J. Plasticity 16 (2000) 225–240.
[19] G. Kang, A visco-plastic constitutive model for ratcheting of cyclically stable materials and its finite element implementation, Mech. Mater. 36 (2004) 299–312.
[20] S. Guo, G. Kang, J. Zhang, A cyclic visco-plastic constitutive model for time-dependent ratchetting of particle-reinforced metal matrix composites, Int. J. Plasticity 40 (2013) 101–125.
[21] M. Abdel-Karim, Modified kinematic hardening rules for simulations of ratchetting, Int. J. Plasticity 25 (2009) 1560–1587.
[22] J. Fred, MINUIT tutorial-function minimization, CERN (2004).